

Supporting Information (SI)

Remote substitutes and coordination anions effect on magnetic properties of Co(II) dimmer complexes

Tong-Kai Luo,^a Xiang Zhong,^a Qing-Yun Zhang,^a Xiao-Feng Chen,^a Hui Xu,^a Yan Peng,^{*a} Sui-Jun Liu,^{*a} Zhao-Bo Hu,^{*ab} and He-Rui Wen^a

^aSchool of Chemistry and Chemical Engineering, Jiangxi Provincial Key Laboratory of Functional Molecular Materials Chemistry, Jiangxi University of Science and Technology, Ganzhou 341000, Jiangxi Province, P. R. China. E-mail: py16882020@163.com (Y. Peng); sjliu@jxust.edu.cn (S.-J. Liu), Tel: +86-0797-8312204.

^bChaotic Matter Science Research Center, Faculty of Materials Metallurgy and Chemistry, Jiangxi University of Science and Technology, Ganzhou 341000, P. R. China. E-mail: huzhaobo@smail.nju.edu.cn (Z.-B. Hu)

Experimental

General information

All chemicals and solvents were obtained from commercial sources without further purification. All reactions were carried out under aerobic conditions. The elemental analyses (C, H, and N) were carried out using an Elementar Vario EL analyzer. Fourier transform IR spectra (4000 to 400 cm^{-1}) were measured on a Perkin-Elmer Spectrum GX spectrometer with samples prepared as KBr discs. Powder X-ray diffraction was carried out on a STOE STADI-P diffractometer, using Cu-K α radiation with $\lambda = 1.5406 \text{ \AA}$. Thermogravimetric analyses (TGA) were carried out on a NETZSCH STA2500 (TG/DTA) thermal analyzer under an inert atmosphere (maintained by a N_2 gas flow) at a heating rate of $10 \text{ }^\circ\text{C min}^{-1}$.

X-ray crystal structures

The crystal structures were determined at room temperature on a Bruker diffractometer with graphite-monochromator Mo-K α radiation. The structures were solved by direct methods and refined by full-matrix least-squares using the SHELXTL program suite.

Physical measurements

Variable-temperature dc magnetic susceptibility measurements and ac magnetic susceptibility measurements were conducted on microcrystalline samples, suspended in eicosane to prevent torquing. Magnetic susceptibility data (2-300 K) were collected on powdered samples using a SQUID-based sample magnetometer, Quantum Design model MPMS-VSM instrument under a 1000 Oe applied magnetic field. Magnetization isotherms were collected at 1.8 K, 2 K, 5 K and 10 K between 0 and 7 T. Ac susceptibility measurements were carried out under an oscillating ac field of 2 Oe and ac frequencies ranging from 1 to 1000 Hz. Data were corrected for diamagnetism using Pascal constants and a sample holder correction.

Synthesis of Ligands

The two ligands were synthesized by same method, therefore only $\text{H}_2\text{L1}$ will be discussed in detail.

$\text{N, N}'\text{-bis}[(2\text{-hydroxybenzylideneamino})\text{-propyl}]\text{-piperazine}$ ($\text{H}_2\text{L1}$)

An ethanol solution containing salicylaldehyde (10 mmol, 1.20 g) was mixed with 1,4-bis (3-aminopropyl) piperazine (5 mmol, 1.00 g) in ethanol. The yellow mixture was refluxed for 8 hours under stirring. The desired yellow product was obtained by slow evaporation of the solution. $\text{H}_2\text{L1}$ ($\text{N, N}'\text{-bis}[(2\text{-hydroxybenzylideneamino})\text{-propyl}]\text{-piperazine}$) Yield: 1.80 g (88% based on 1,4-bis (3-aminopropyl) piperazine). Anal. calc. (%) for $\text{C}_{24}\text{H}_{32}\text{N}_4\text{O}_2 \cdot 2\text{H}_2\text{O}$ (444.57): C, 64.84; H, 8.16; N, 12.60 wt %; found: C, 64.74; H, 8.23; N, 12.87 wt %. $^1\text{H NMR}$ (400 MHz, CDCl_3) δ 13.56 (s, 2H), 8.35 (s, 2H), 7.35-7.27 (m, 2H), 7.24 (dd, $J = 7.7, 1.7 \text{ Hz}$, 2H), 6.96 (dd, $J = 8.3, 1.0 \text{ Hz}$, 2H), 6.88 (td, $J = 7.5, 1.1 \text{ Hz}$, 2H), 3.64 (td, $J = 6.8, 1.2 \text{ Hz}$, 4H), 2.43 (d, $J = 7.7 \text{ Hz}$, 12H), 1.89 (p, $J = 6.9 \text{ Hz}$, 4H). FT-IR (KBr, cm^{-1}): 3742 (w), 3679 (w), 3054 (w), 2934 (m), 2809 (m), 1633 (vs), 1499 (m), 1453 (m), 1345 (w), 1280 (s), 1204 (w), 1144 (m), 970 (w), 889 (m), 755 (s), 640 (w).

$\text{N, N}'\text{-bis}(2\text{-hydroxy-5-bromobenzyl})\text{-1,4-bis}(3\text{-iminopropyl})\text{-piperazine}$ ($\text{H}_2\text{L2}$)

The synthesis of $\text{H}_2\text{L2}$ is the same as that of $\text{H}_2\text{L1}$ by replacing the salicylaldehyde to 5-bromosalicylaldehyde. Yield: 1.90 g (67% based on 1,4-bis (3-aminopropyl) piperazine). Anal. calc. (%) for $\text{C}_{24}\text{H}_{30}\text{Br}_2\text{N}_4\text{O}_2$ (566.33): C, 50.90; H, 5.34; N, 9.89 wt %; found: C, 50.90; H, 5.00; N, 10.10 wt %. $^1\text{H NMR}$ (400 MHz, CDCl_3) δ 13.60 (s, 2H), 8.28 (s, 2H), 7.37 (dt, $J = 5.5, 2.4 \text{ Hz}$, 4H), 6.86 (d, $J = 8.7 \text{ Hz}$, 2H), 3.66 (t, $J = 6.7 \text{ Hz}$, 4H), 2.89-2.21 (m,

12H), 1.94-1.82 (m, 4H). FT-IR (KBr, cm^{-1}): 3743 (s), 3676 (w), 3617 (w), 2934 (m), 2811 (m), 2765 (w), 1695 (w), 1636 (s), 1517 (w), 1478 (w), 1365 (m), 1274 (s), 1165 (w), 969 (w), 825 (s), 627 (w).

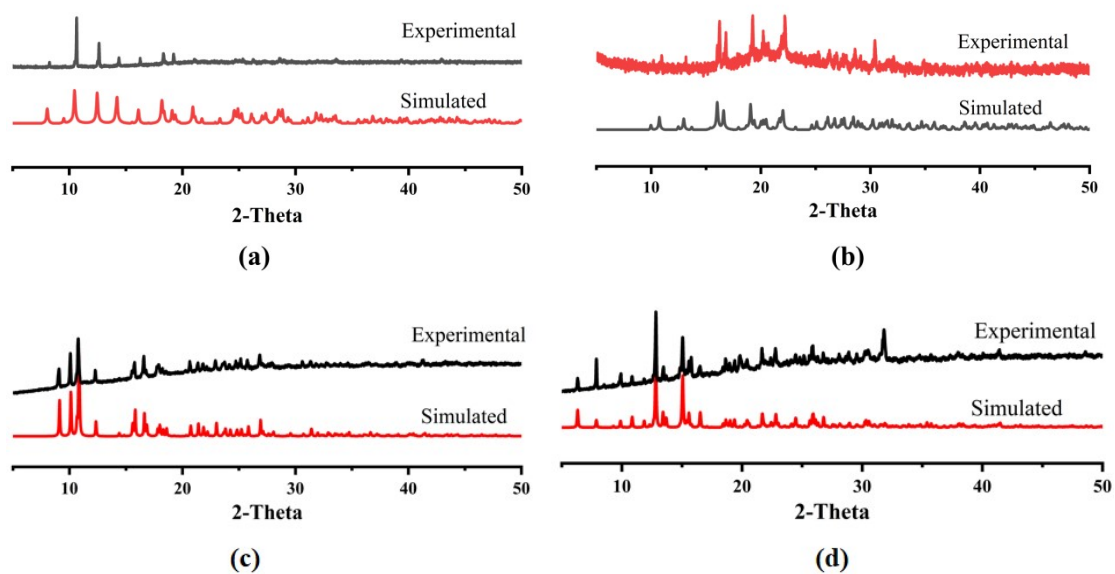


Fig. S1 Powder X-ray diffraction data for 1-4 (a-d).

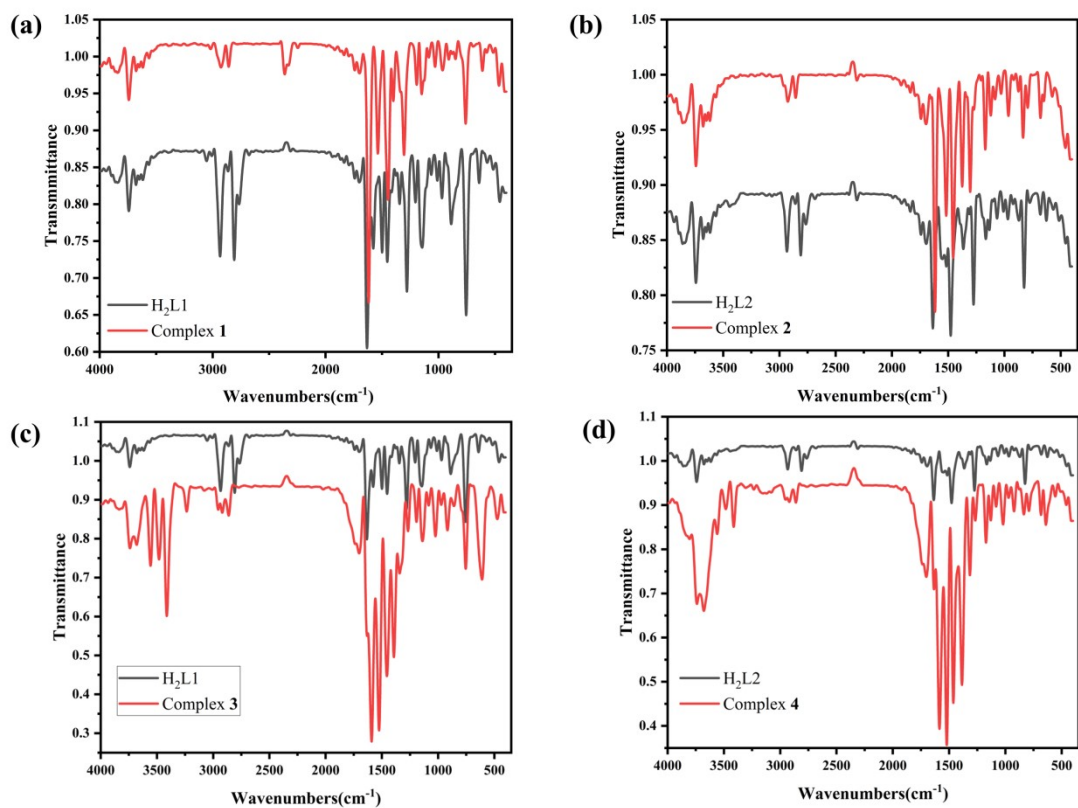


Fig. S2 IR spectroscopy of complexes 1-4 (a-d)

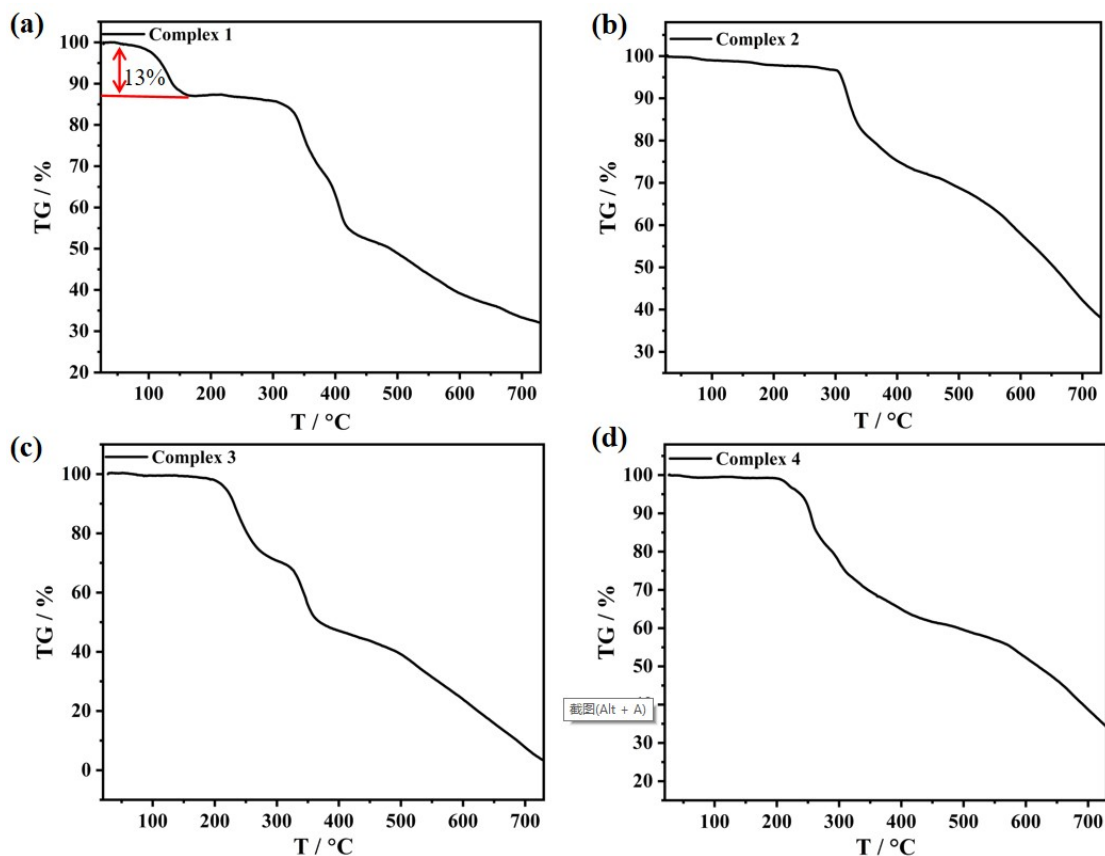


Fig.S3. TGA plots of complexes 1-4 (a-d).

Table 3. Continuous Shape Measures (CShMs) of the coordination geometry for Co(II) ion in complexes 1-4.

Complexes	Label	Shape	Symmetry	Distortion
1	SP-4	Square	D _{4h}	25.2098
	T-4	Tetrahedron	T _d	2.0319
	SS-4	Seesaw	C _{2v}	7.1444
2	SP-4	Square	D _{4h}	27.3930
	T-4	Tetrahedron	T _d	1.7353
	SS-4	Seesaw	C _{2v}	7.8209
3	PP-5	Pentagon	D _{5h}	34.03126
	vOC-5	Vacant octahedron	C _{4v}	5.75785
	TBPY-5	Trigonal bipyramid	D _{3h}	0.36928
	SPY-5	Spherical square pyramid	C _{4v}	3.77594
	JTBPY-5	Johnson trigonal bipyramid J12	D _{3h}	3.18736
4	PP-5	Pentagon	D _{5h}	33.28680
	vOC-5	Vacant octahedron	C _{4v}	3.87570
	TBPY-5	Trigonal bipyramid	D _{3h}	1.04673
	SPY-5	Spherical square pyramid	C _{4v}	2.36315
	JTBPY-5	Johnson trigonal bipyramid J12	D _{3h}	3.52584

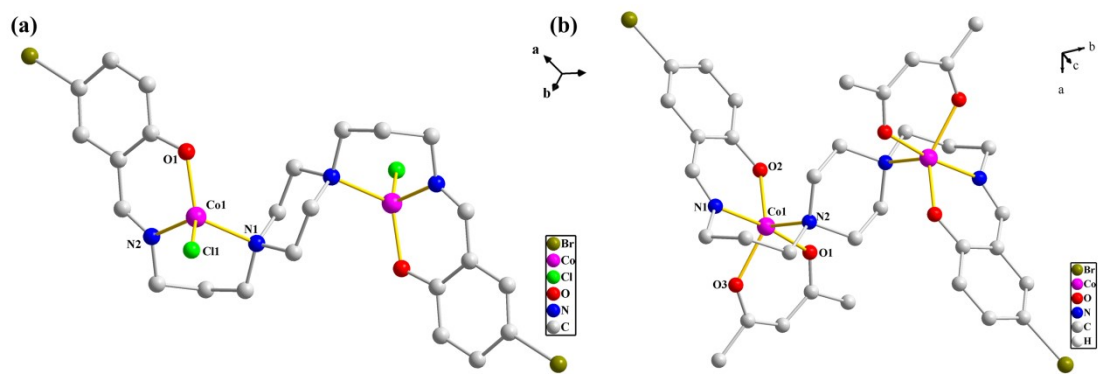


Fig. S3 Molecular structures of complexes **2** and **4** (left and right)

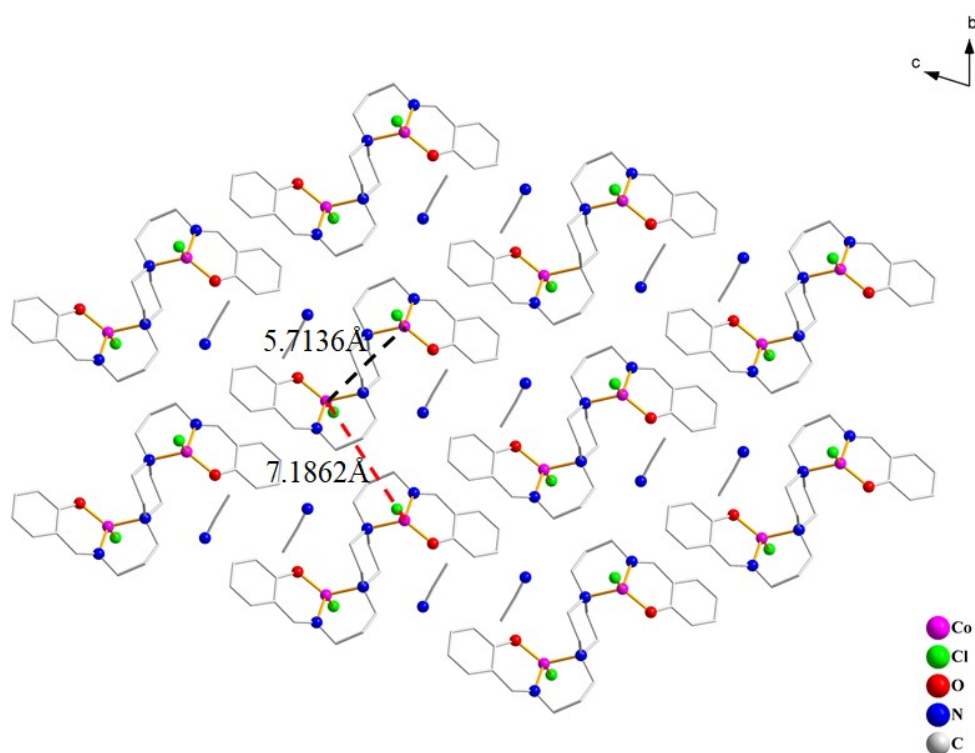


Fig. S5 Packing of complex **1**. dash lines are the intramolecular Co-Co distances (black dash line) and intermolecular Co-Co (red dash line) distances withing the complex.

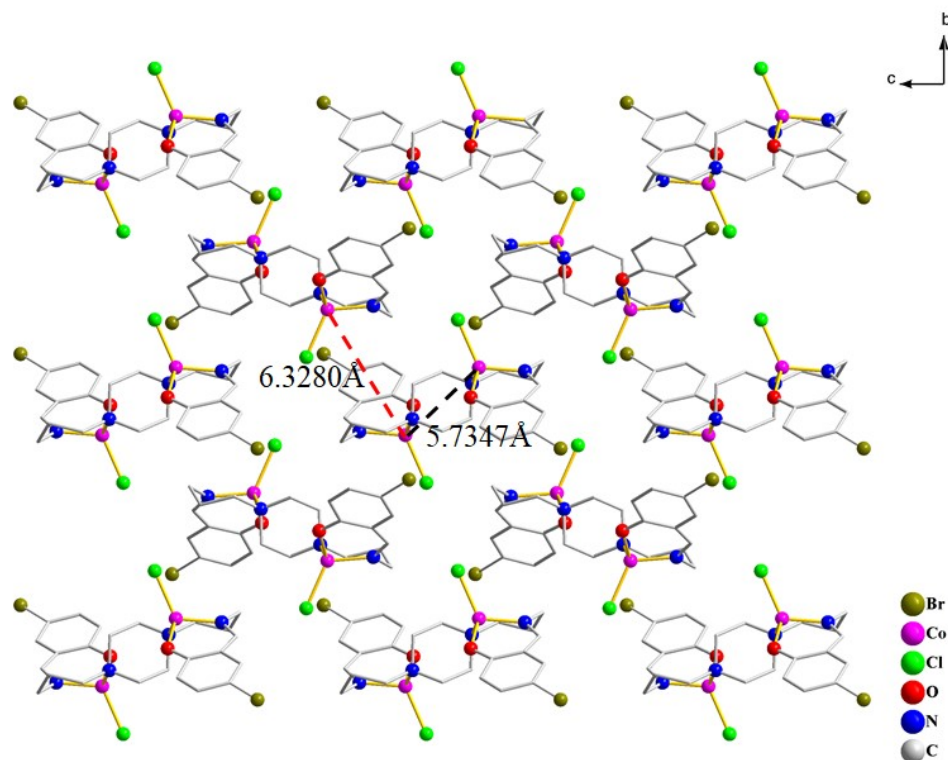


Fig. S6 Packing of complex 2. dash lines are the intramolecular Co-Co distances (black dash line) and intermolecular Co-Co (red dash line) distances within the complex.

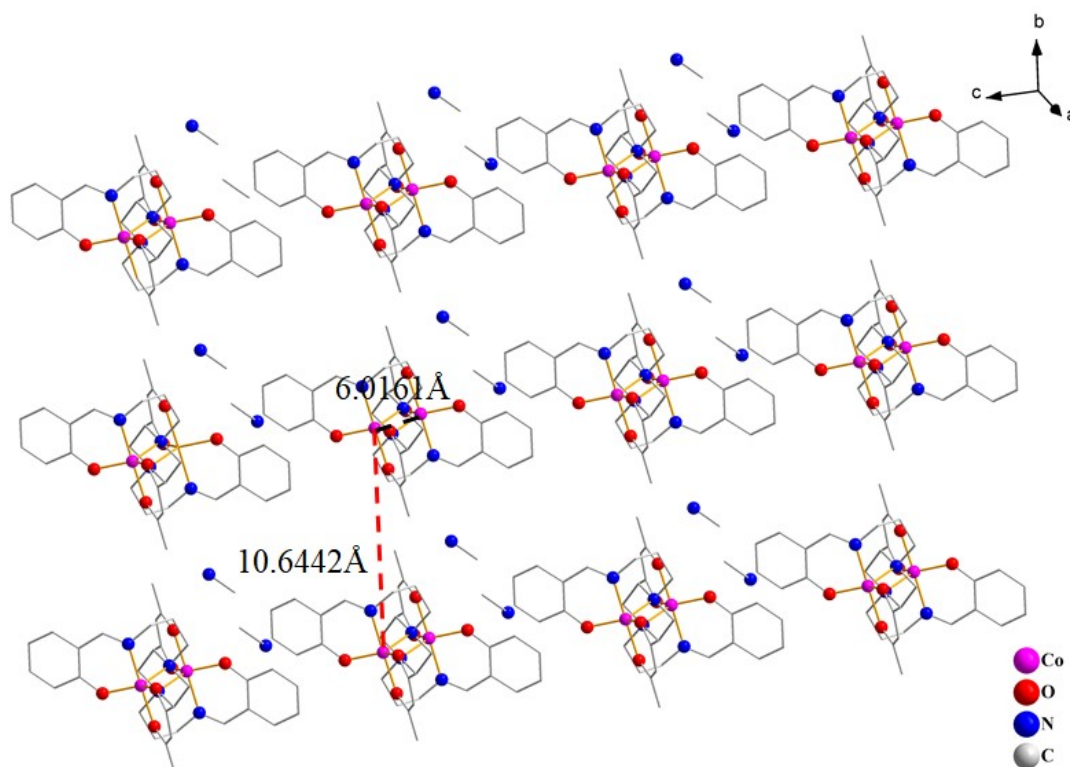


Fig. S7 Packing of complex 3. dash lines are the intramolecular Co-Co distances (black dash line) and intermolecular Co-Co (red dash line) distances within the complex.

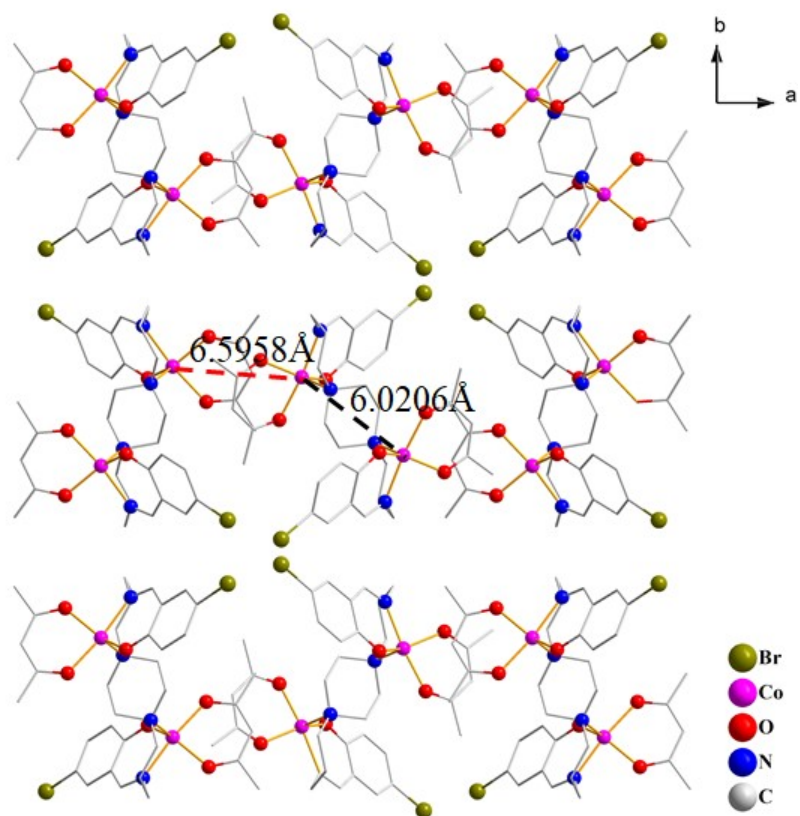


Fig. S8 Packing of complex 4. dash lines are the intramolecular Co-Co distances (black dash line) and intermolecular Co-Co (red dash line) distances within the complex.

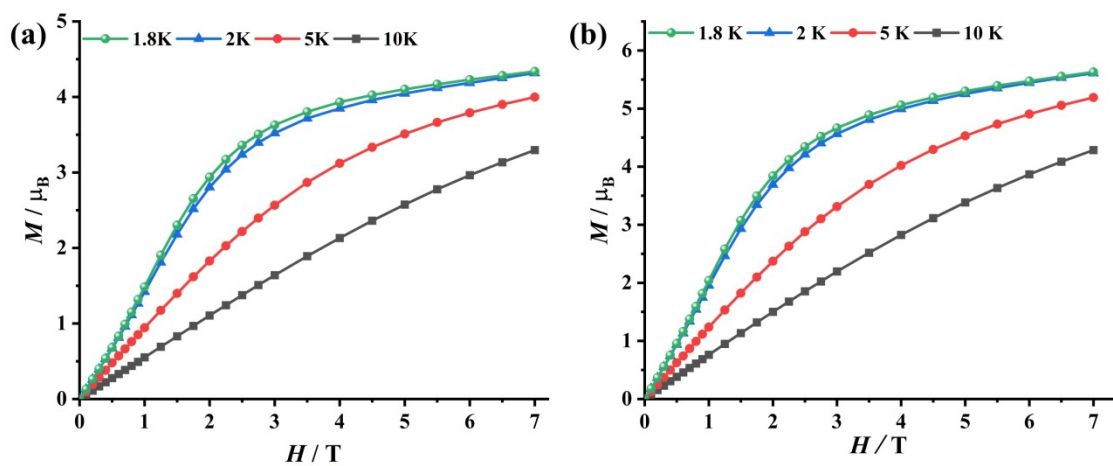


Fig. S9 Plots of M vs H at different temperature for complexes 1 and 2 (left to right)

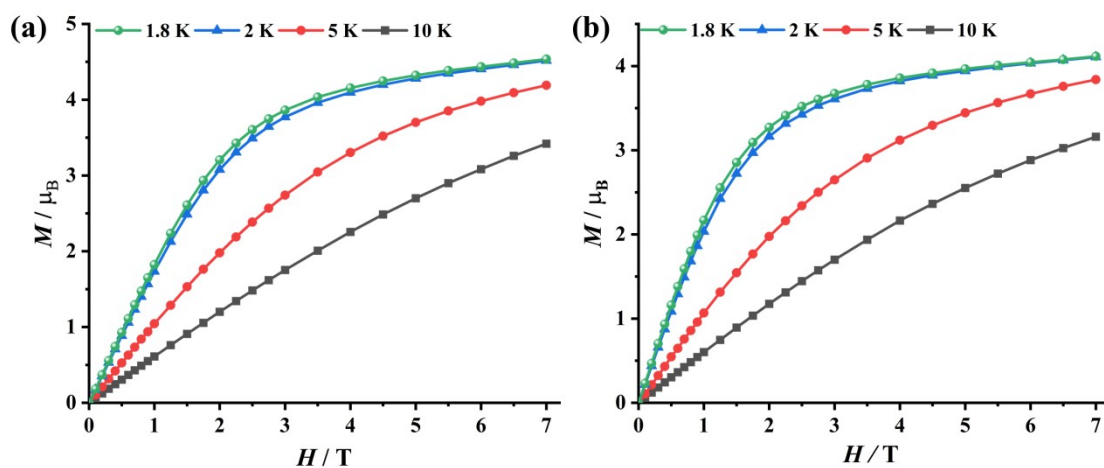


Fig. S10 Plots of M vs H at different temperature for complexes **3** and **4**(left to right)

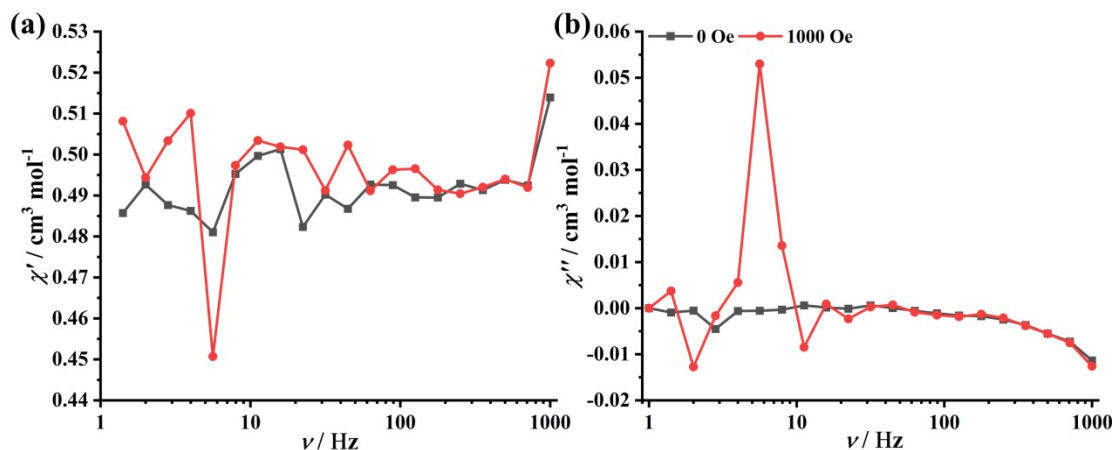


Fig. S11 Plots of χ' (left) and χ'' (right) vs frequencies at 2 K in different dc fields for complex **2**

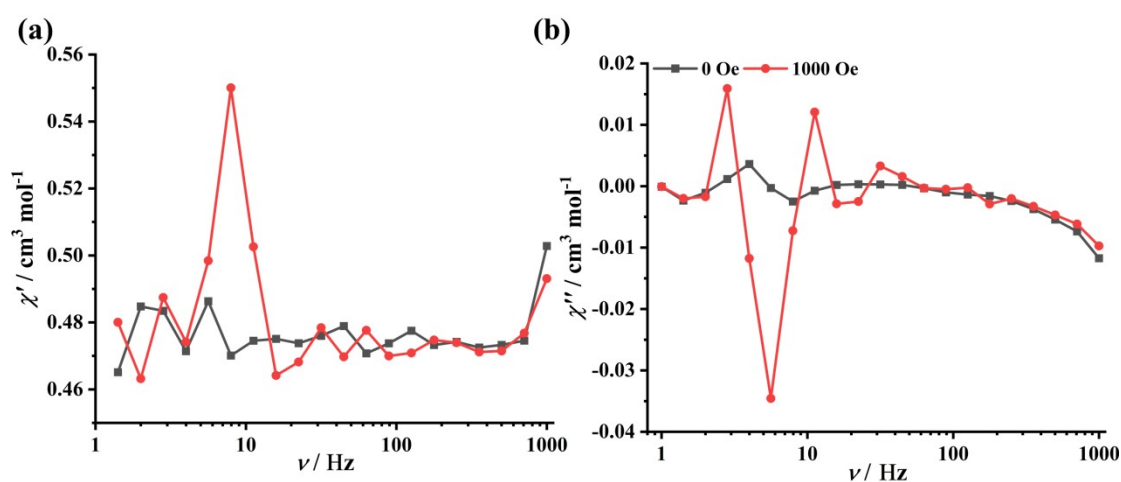


Fig. S12 Plots of χ' (left) and χ'' (right) vs frequencies at 2 K in different dc fields for complex **3**

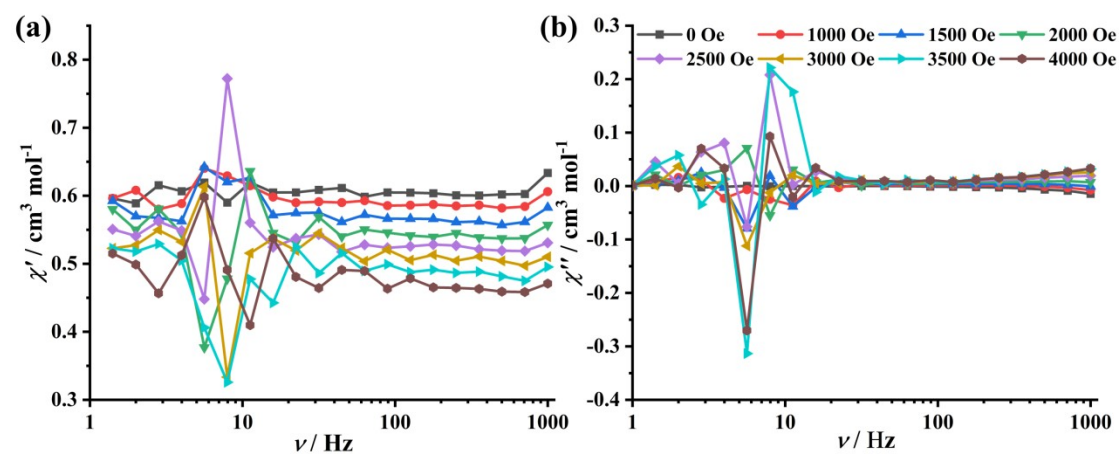


Fig. S13 Plots of χ' (left) and χ'' (right) vs frequencies at 2 K in different dc fields for complex **4**